The design layout of the MEMS S&A interrupter device is shown in Figure 4-6, with an accompanying SEM image of the fabricated device shown in Figure 4-7.

While all of the key interrupter components (plates, actuators, and latches) are important to its proper functioning, the actuators have the most design parameters that need to be considered. By comparison, the plates are relatively simple structural components that are linked to the actuators by a fixed beam, and the latches are essentially fixed structures that enable locking by physically mating with an extension of the actuators. In the following section, some of the analysis that went into the design of the electrothermal actuator will be discussed.

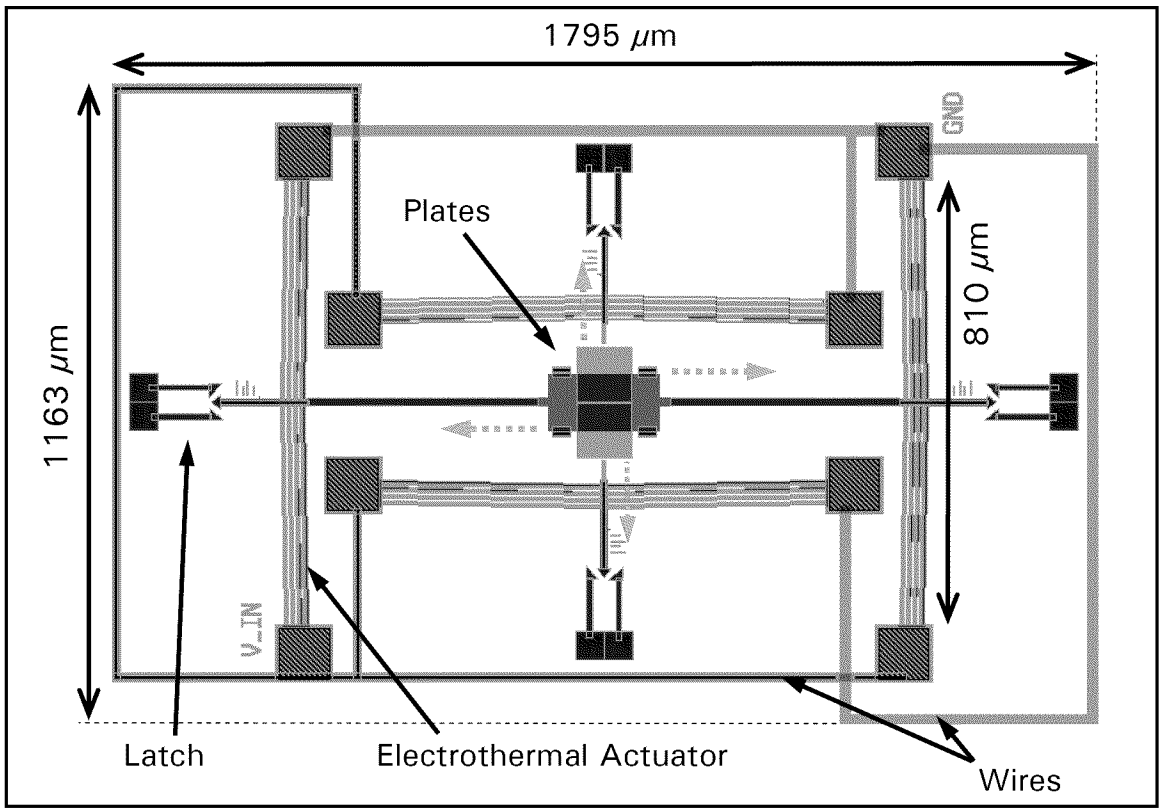


Figure 4-6. Design layout of the entire MEMS S&A interrupter device. The green arrows in the center represent the direction of motion upon actuation. The entire device covers an area less than 2.1 mm².

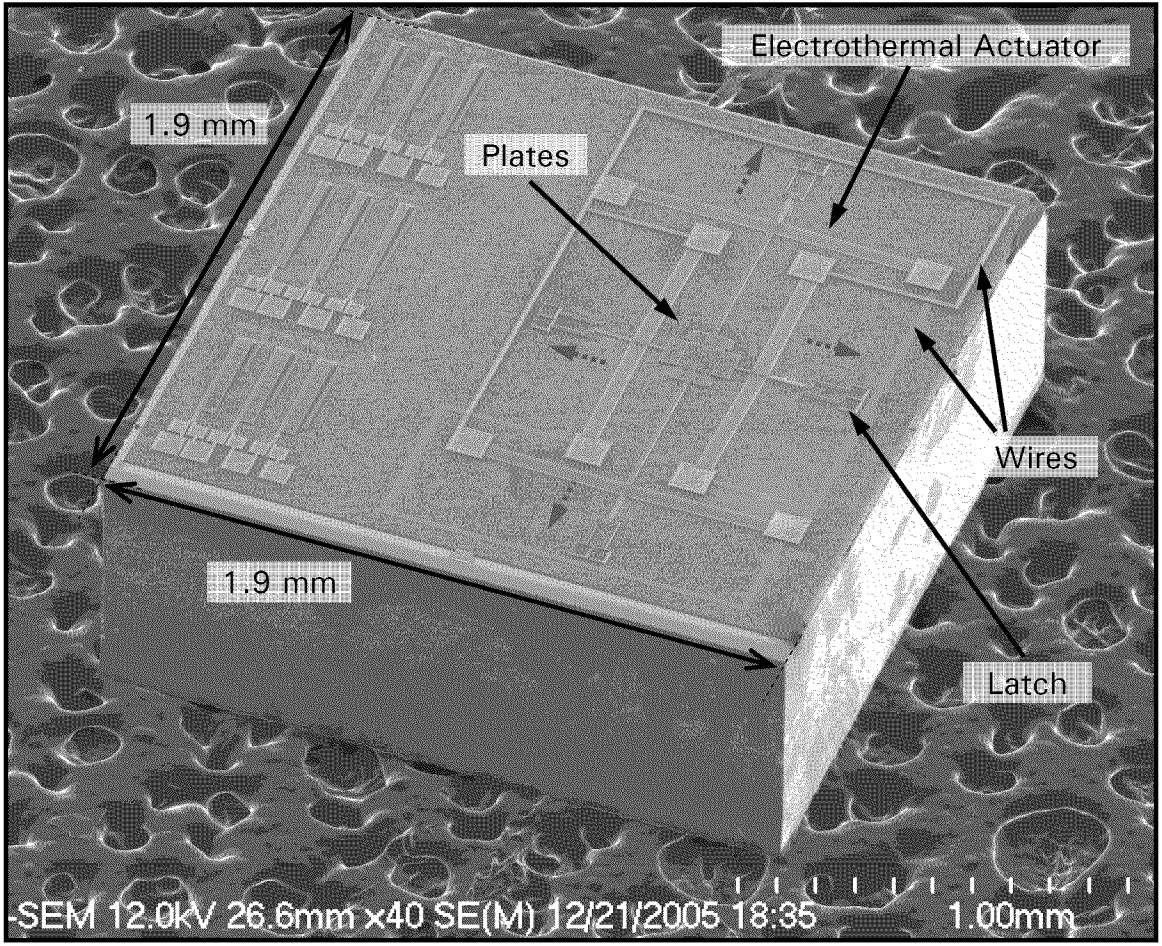


Figure 4-7. SEM image of the fabricated MEMS S&A interrupter device from the design layout shown in Figure 4-6. Again, the green arrows represent the direction of actuator motion when power is applied. Also, note that the entire device is smaller than the 3.8 mm² die.

4.3 Electrothermal Actuator Theory

All electrothermal actuators operate on the principles of Joule heating and thermal expansion. Joule heating is the increase in temperature that occurs due to a material's resistivity when a current flows through that material [5]. In general, the actuator is designed such that at least one arm (or length of material) has the proper dimensions to induce a large enough current density to cause the arm to expand as a result of the increase in temperature. As this arm expands, the entire device is forced to move in a specific direction, dependent on the arrangement of the structure and the location of its

anchored (fixed) ends. The two types of electrothermal actuators considered for the interrupter mechanism were the standard u-shaped actuator and the bent-beam actuator. The geometry of the u-shaped actuator causes it to deflect in an arcing motion, while the bent-beam actuator's geometry causes it to deflect in a linear direction. The motion of both actuators is in-plane with the substrate. Figure 4-8 shows a simple illustration of both electrothermal actuators. Note that the bent-beam actuator in Figure 4-8(b) is shown with four expanding arms (two on each side), and that the number of arms is considered a design parameter for optimizing the actuator.

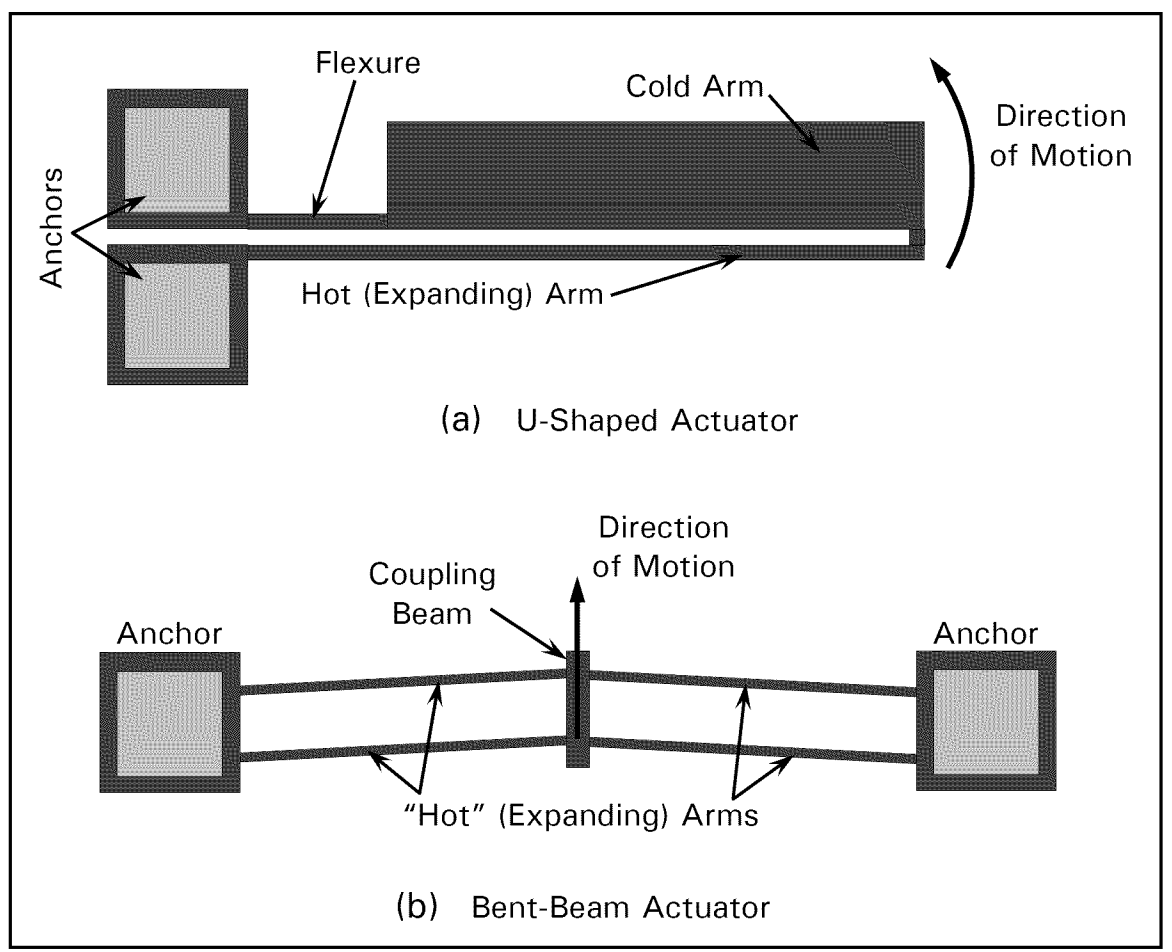


Figure 4-8. Simple schematics of two electrothermal actuators considered for use with the interrupter mechanism fabricated in this research effort. (a) U-shaped actuator showing in-plane arcing motion. (b) Bent-beam actuator showing linear in-plane motion.

4.3.1 Thermal Expansion Theory

To describe the expansion of a material due to Joule heating, look at the beam in Figure 4-9 [6]. The original beam length is L_0 , the expansion as a result of Joule heating is ΔL , and the length of the beam after thermal expansion is L_{new} . Therefore:

$$L_{new} = L_0 + \Delta L \quad (\mu \text{m}) \tag{4.1}$$

Furthermore, all materials have a coefficient of (linear) thermal expansion, α_L , that is used to quantify the relative linear change in an object as a result of a change in temperature, ΔT [7]. This relationship can be expressed as:

$$\alpha_L = \frac{\Delta L}{L} \frac{1}{\Delta T} \quad (K^{-1}) \tag{4.2}$$

Consequently, the expansion due to Joule heating, ΔL , can be described by:

$$\Delta L = \alpha_I \cdot L \cdot \Delta T \quad (\mu m) \tag{4.3}$$

In addition, if the final temperature of the beam is approximated as an average temperature, T_{ave} , and the initial temperature of the beam is T_0 , then Equation (4.1) becomes:

$$L_{now} = L_0 + \alpha_I \cdot L \cdot (T_{ove} - T_0) \quad (\mu m) \tag{4.4}$$

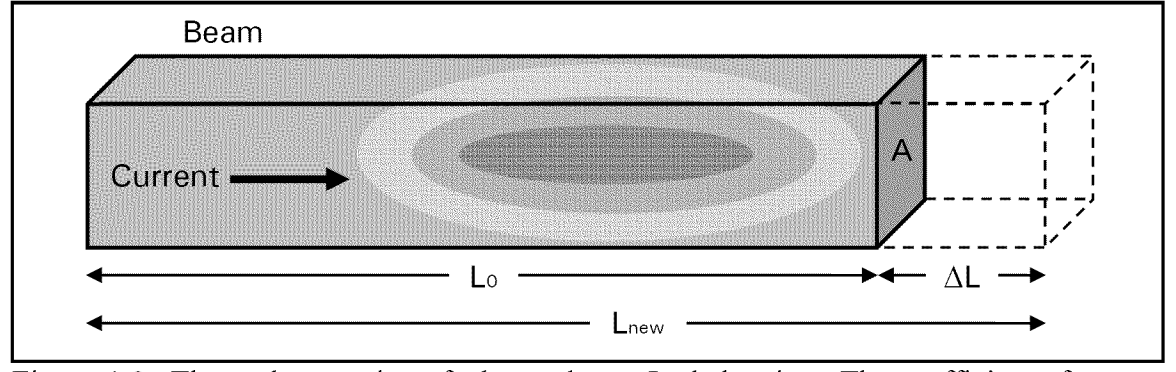


Figure 4-9. Thermal expansion of a beam due to Joule heating. The coefficient of thermal expansion associated with the specific beam material will be a key factor in determining the change in length. The other contributing factor is the current per cross-sectional area, A, that will produce a temperature change throughout the beam [6], [7].

The motion in electrothermal actuators is a result of the beam expansion that occurs when sufficient current density is present. Note that the expanding arms in the MEMS actuators shown in Figure 4-8, have a cross-sectional area, A, on the order of 10 μ m². For reference, the coefficient of thermal expansion for polysilicon, which is the material used to fabricate the electrothermal actuators investigated in this thesis, has been reported to be 2.33×10^{-6} K⁻¹ [7], [8].

4.3.2 Electrothermal Actuator Performance Considerations

One of the main benefits of electrothermal actuators is their low operating voltage, which makes them compatible with standard microelectronics circuitry – e.g., complementary metal-oxide-semiconductor (CMOS) devices. Clearly, a goal for any MEMS designer should be the integration of the electronics required for operation to be fabricated on the same die. Another benefit of electrothermal actuators is that their lateral motion is in the same plane as the substrate, and thus it is relatively simple to move other surface micromachined mechanisms by connecting them to these actuators [9]. Additionally, electrothermal actuators have been shown to reliably produce deflections and forces with magnitudes of approximately 15 µm and 10-100 µN, respectively [8], [10], [11]. In contrast to other types of MEMS actuators, for example, electrostatic actuators, which operate at high voltages, produce considerably smaller forces, and are usually limited to only a few micrometers of vertical deflection [12]. Nevertheless, a major drawback to electrothermal actuators is that they consume considerably more power than electrostatic actuators. However, this drawback is usually tolerated for the enhanced in-plane performance.

4.3.3 Electrothermal Actuator Comparisons

The following sections discuss the operation of the two electrothermal actuators – u-shaped and bent-beam – considered for use with the interrupter mechanism.

U-Shaped Actuator

The basic operation of the u-shaped electrothermal actuator can be described by referring to Figure 4-8(a). When a voltage is applied across the two anchors, a current that is dependent on the resistance of the actuator is passed through the actuator. Since the hot arm has a smaller cross-sectional area than the cold arm, it has a larger current density. As a result, the hot arm heats up more than the cold arm, which produces a proportionally larger thermal expansion of the hot arm. This difference in expansion between the two arms causes the actuator tip to deflect in an arcing motion about the anchored end of the cold arm [10], [13].

Furthermore, by maximizing the temperature difference between the hot and cold arms the efficiency of the actuator can be increased. Several techniques available to increase this temperature difference are: 1) increasing the thickness of the cold arm thus reducing its current density, and 2) increasing the width of the cold arm such that more surface area is available to dissipate heat [14]. In fact, any heat dissipated in the flexure or cold arm is considered wasted power since it does not contribute to the actuator's deflection [13]. Clearly, the dimensions for the various elements (hot arm, cold arm, and flexure) of the u-shaped actuator are important design parameters that can be tailored to maximize a particular desired performance, such as deflection, force, or power consumption.

For example, increasing the actuator's overall length tends to increase the total deflection. However, the trade-off is an increase in power consumption since the voltage must increase to compensate for the increased resistance. In addition, the force of the actuator tends to decrease with increasing length. Alternatively, decreasing the width of the flexure will maximize deflection since the actuator is easier to bend as the hot arm expands. However, if the flexure is narrower than the hot arm, it may thermally fail before the hot arm generates any meaningful deflection. Also, increasing the length of the flexure tends to increase deflection; however, this increases power consumption in the flexure and expansion may result, thus counteracting any deflection due to the hot arm Another technique involves increasing the thickness of the actuator to expanding. generate more force, but the larger cross-sectional area of the hot arm will increase the power consumption of the device. The final technique is increasing the hot arm width to a value slightly greater than the thickness in order to maximize force, while again sacrificing a slight increase in power consumption [11], [13], [14]. For illustrative purposes, Figure 4-10 shows a deflection versus input power curve for a typical u-shaped electrothermal actuator. The specific dimensions for this actuator are given in the figure.

Bent-Beam Actuator

The basic operation of the bent-beam electrothermal actuator can be described by referring to Figure 4-8(b). When a current is passed through the "hot" arms by an applied voltage across the two anchors, the arms tend to lengthen as a result of thermal expansion. The cross-sectional area of the arms is designed to be very small (on the order of 1 μ m²) in order to ensure a sufficient current density is obtained such that the arms thermally expand, as previously discussed. Furthermore, pairs of identical arms are

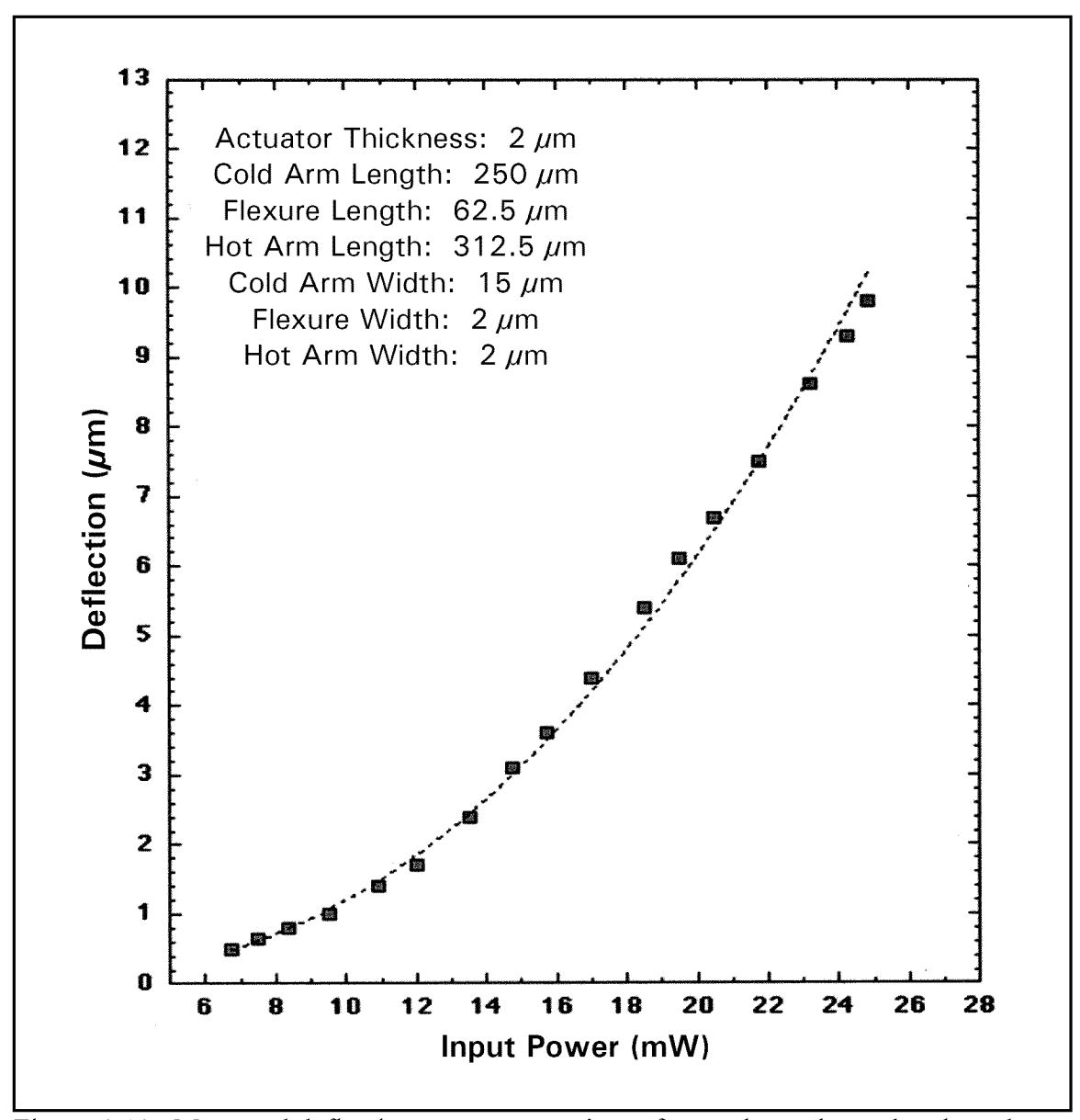


Figure 4-10. Measured deflection versus power input for an electrothermal u-shaped actuator fabricated in the PolyMUMPs process. Data points come from five identical actuators [13].

coupled by a beam placed in the center of the actuator. Since the arms are fixed by the anchors, the bent-beam actuator will move linearly as the arms expand. This linear movement due to the coupling beam provides a method to transmit the resulting linear force to another device, in addition to adding structural integrity to the actuator. To

ensure the expanding arms bend in the desired direction, the actuator is designed with a small pre-bend angle. The location of the pre-bend angle, θ , and the arm length, L, as used in this thesis are defined in Figure 4-11 [8].

The performance of the bent-beam actuator (e.g., deflection distance and force) can be optimized by varying the following design parameters: the number of arm pairs; the arm length; the pre-bend angle; and the actuator thickness. For example, the deflection of the actuator is dependent on the arm length and the pre-bend angle, but independent on the number of arm pairs and the actuator thickness. In addition, the deflection is directly related to the drive voltage, which, as expected, will result in an increase in current density. Obviously, there is a limit at which the current density will exceed the carrying capability of the arms and the device will catastrophically fail. As another example, the force of the actuator is directly proportional to the number of arm pairs and the actuator thickness, as well as the pre-bend angle [8]. Moreover, Que et al showed that a linear relationship exists between the actuator deflection and generated output force, such that the force of the bent-beam actuator decreases as the deflection increases [15].

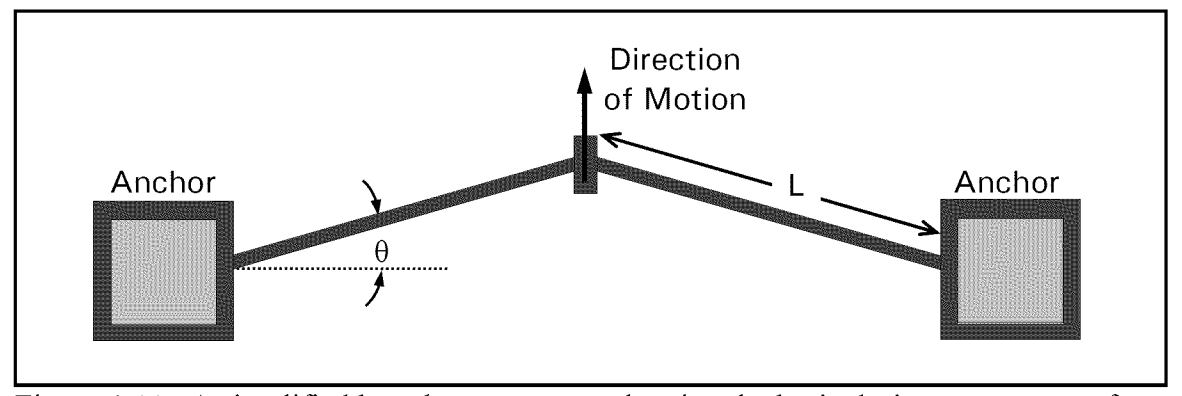


Figure 4-11. A simplified bent-beam actuator showing the basic design parameters of pre-bend angle, θ , and arm length, L. Note: that θ is exaggerated for illustrative purposes.

4.3.4 Electrothermal Actuator Designed for Interrupter Mechanism

Between the two electrothermal actuators discussed above, the bent-beam actuator was chosen to provide the actuation forces for the interrupter mechanism designed in this research effort. A number of factors contributed to this choice, but the desire to have the four interrupter plates separate themselves in a linear motion, was the most significant. The linear motion reduces the complexity of the interruption method and simplifies the implementation of the actuation, thereby increasing reliability. Implementation of the interrupter mechanism using the u-shaped actuator is more complex, because of its inherent arcing motion. While it is true that several u-shaped actuators can be designed with a common yoke, to provide a linear force, this type of linkage tends to significantly reduce the amount of force that can be delivered [8]. Clearly, this type of force reduction does not exist for the bent-beam actuator. It is worth noting that Comtois et al. investigated a creative rotary yoke design to be used with u-shaped actuators, however, this type of design requires a fabrication process with at least three releasable layers [16].

Another reason for selecting the bent-beam actuator was the larger output force available, which would be beneficial in rapidly separating the interrupter plates to create an opened path for the flyer material. The bent-beam actuator has a large force output because of the increased number of arms that can be added to its design [8]. However, it must be keep in mind that increasing the force by adding additional arms will also result in a decrease in deflection. This larger force may be advantageous if increasing the dimensions (and consequently the mass) of the interrupter plates is desirable. The next section will address specific design parameters selected for the bent-beam electrothermal actuator used in this research.

4.4 Bent-Beam Electrothermal Actuator

The primary objectives considered in selecting the design parameters for the bent-beam electrothermal actuators included: 1) ensure enough force was available to completely separate the four interrupter plates, and 2) provide the greatest amount of deflection to maximize the dimensions of the opened area. The force requirement was critical since the actuators must provide enough force to move the plates a reasonable distance. If this could not be accomplished, the entire interrupter mechanism would be ineffective. With the above goals in mind, the main design parameters of actuator thickness, the number of arm pairs, the length of the arm, and the pre-bend angle were chosen to optimize the actuator's performance. Additionally, various test structures were designed to characterize the true performance of the fabricated actuators.

4.4.1 Design Parameter Optimization

To ensure the force requirement was satisfied, the first parameter considered was the actuator thickness. PolyMUMPs offers three different thickness possibilities for its releasable layers: 1.5 µm (Poly2), 2.0 µm (Poly1), and 3.5 µm (Poly1 + Poly2). As described in section 4.3.3, an increase in actuator thickness will produce an increase in output force [8]. Therefore, the actuator was chosen to be the maximum thickness of 3.5 µm. Although the additional thickness is only required for the expanding arms, the entire actuator was designed to be 3.5-µm thick in order to maintain structural integrity. The only drawback from the increased thickness is an increase in power consumption due to the larger current density required to thermally expand the arms.

The second design parameter that can increase the output force is to increase the number of arm pairs. However, the maximum force occurs when the deflection is small,

and decreases linearly as the deflection continues to increase [15]. Therefore, since maximizing deflection is also desirable and deflection is dependent on arm length, a balance between arm length, and the number of arm pairs had to be considered. The selection for these design parameters was based on experimental data from a previously successful bent-beam actuator design. Szabo experimented with multiple bent-beam actuator designs that varied both the arm length and the number of arm pairs, while keeping the thickness of the arms constant at 3.5 µm [17]. A summary of the measured data he obtained is shown in Table 4-1. Observe that a maximum deflection of 19 µm was observed from the 350 μ m \times 8 arm (arm length \times number of arm pairs) bent-beam actuator. However, it must be noted that this actuator required a relatively large input power when compared to the other actuator designs. A large power requirement was also necessary for the 350 μ m \times 16 arm and the 400 μ m \times 12 arm actuators. This could be expected due to the decreased parallel resistance provided by additional arm pairs that effectively reduces the current in each path for a given voltage. Clearly, a reasonable compromise between deflection and power is offered by the 400 μ m \times 8 arm actuator. Thus, the 400 μ m \times 8 arm actuator was chosen to provide the necessary actuation force for one of the three interrupter mechanisms designed in this thesis. For comparative purposes, a second interrupter mechanism with 400 μ m \times 12 arm actuators was designed.

In addition to arm length, the deflection of the bent-beam actuator is dependent on the pre-bend angle. Figure 4-12 shows the deflection versus pre-bend angle for a series of 2-µm thick polysilicon bent-beam actuators as presented by Sinclair [8]. The figure clearly shows that a pre-bend angle of 1.05° produced the most deflection. Furthermore, note that the deflection dramatically decreases as the pre-bend angle decreases from

1.05°. Sinclair also observed that for very small pre-bend angles the actuator bends in the vertical direction, and no longer provides in-plane actuation [8]. The pre-bend angle for the actuators tested by Szabo was approximately 1.0° [17], so it was for these reasons that a pre-bend angle of 1.05° was chosen for this research effort.

Table 4-1. Summary of the bent-beam actuators tests described by Szabo [17].

Bent-Beam Actuator Design Parameters (Arm Length × No. of Arm Pairs)	Maximum Input Power at Ma Deflection (μm) Deflection (mW)	
250 μm × 8 arm	12.5	350
350 μm × 8 arm	19.0	775
350 μm × 16 arm	16.0	690
400 μm × 4 arm	16.0	320
400 μm × 8 arm	16.5	360
400 μm × 12 arm	16.5	880

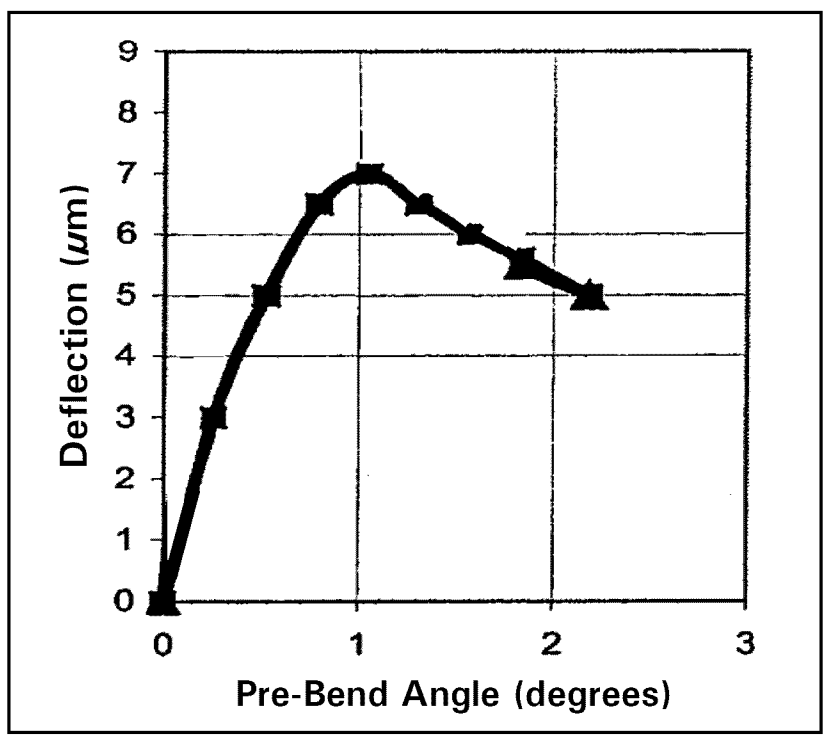


Figure 4-12. Results of deflection versus pre-bend angle tests performed on 2- μ m thick polysilicon bent-beam electrothermal actuators [8]. The maximum deflection was observed for a pre-bend angle of 1.05°.

As a final attempt to maximize the performance of the bent-beam actuators, a third interrupter mechanism was designed with arms that were thicker in the middle than at the ends. This tapered design was investigated by Sinclair in an effort to increase the actuator's thermal power limits, and thus produce an improved mechanical output, in terms of increased deflection and force. For a straight design, the temperature profile is heavily dependent on the inherent heat sinks provided by the anchors at both ends of the actuator and the coupling beam that is geometrically centered between the arm pairs. By adding extra material at the center of the arm (where most of the heat is generated), the heat dissipation at that location is improved. As a result of the tapered design, the temperature over the length of the arm is more evenly distributed, thus reducing the probability of thermal failure [18]. Figure 4-13 shows the temperature distribution profile for two bent-beam actuators – one with straight arms and one with tapered arms. Notice that the maximum temperature for the tapered design (named P1-ST, for Poly1 – symmetric tapered) is distributed more evenly over the length of the arm. The arm length in both actuators is 220 μm, and the overall actuator length is approximately 460 μm.

To optimize both the force and deflection, it is desirable that these electrothermal actuators operate near their thermoelastic limit, which for polysilicon is around 1173 - 1273 K [18]. The thermoelastic limit is the maximum point at which polysilicon cools due to the thermoelastic effect, which occurs when a tensile load (or, in this case, arm expansion) is experienced. At temperatures above this limit, additional heating occurs due to its thermal expansion [19], and thermal failure of the actuator rapidly follows. For reference, note that the melting point of polysilicon is 1685 K. (This value is actually for bulk single-crystal silicon; but it does provide a reasonable approximation [20].)

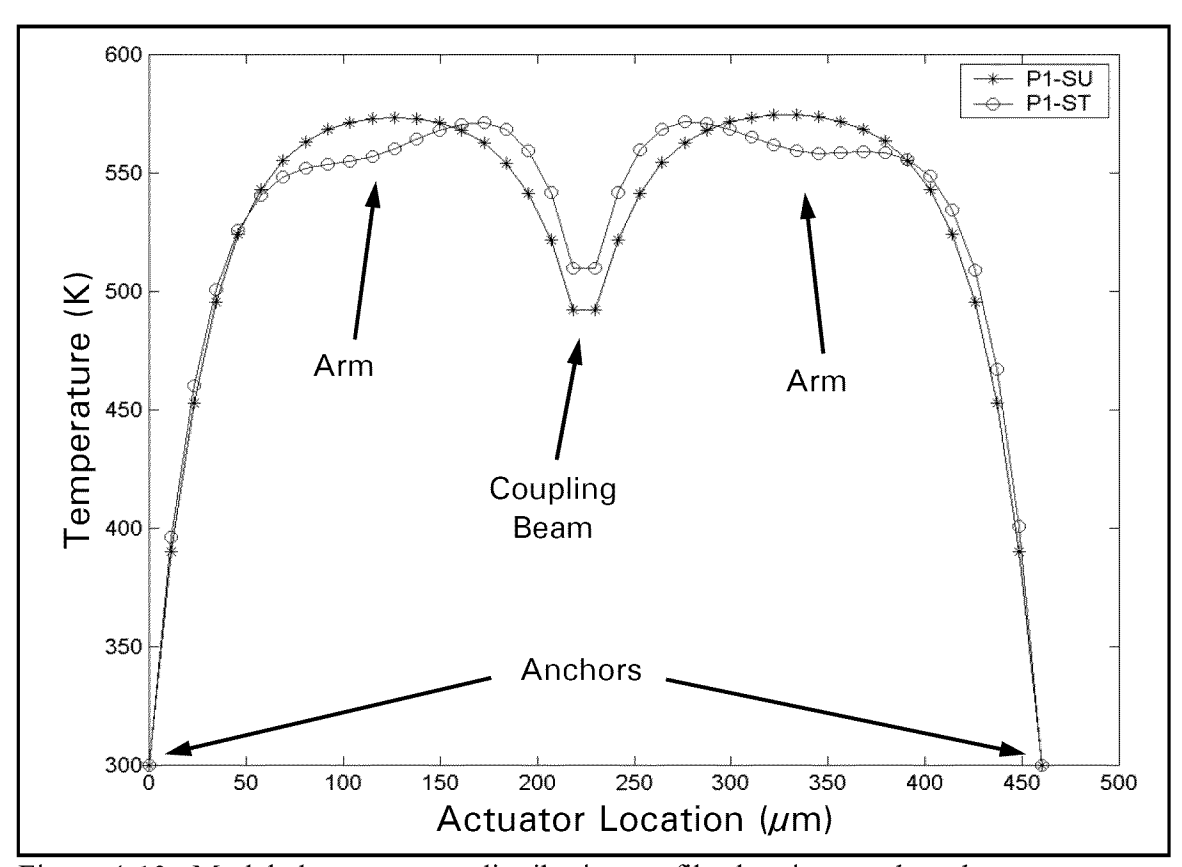


Figure 4-13. Modeled temperature distribution profile showing two bent-beam actuators – straight arms (P1-SU) and tapered arms (P1-ST) [18]. The more evenly distributed temperature over the length of the tapered arm is evident. Note, the length of the arms in both actuators is 220 μ m, making the overall actuator length approximately 460 μ m.

The naming convention used to define the tapered arm geometry is shown in Figure 4-14(a), along with a graphical representation of the deflection versus the C/D tapering ratio [18] in Figure 4-14(b). Using this data, a third interrupter mechanism was designed using the 400 μ m \times 8 arm bent-beam actuators with a C/D tapering ratio of 1.32 in order to maximum deflection. This will enable the observation of any performance improvements that result from this tapered design. A series of stand-alone bent-beam actuators were also designed so individual performance data could be obtained. Any performance relationships that exist between the individual actuators, and that of the entire interrupter mechanisms, will be examined and discussed in Chapter 5.

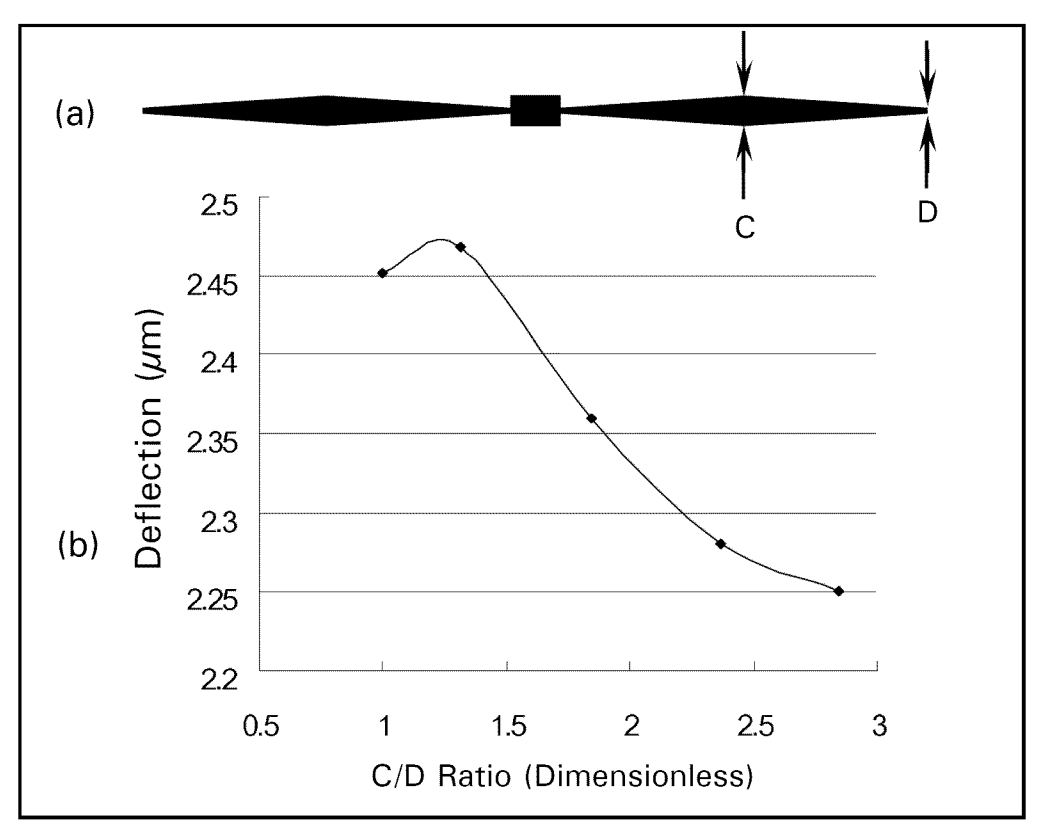


Figure 4-14. (a) Illustration of a hot arm pair that shows the naming convention used to define the tapering geometry. (b) Simulated deflection curve as a function of the C/D ratio. Note: maximum deflection is produced by a C/D ratio of 1.32 [18].

To summarize, three different sets of bent-beam electrothermal actuators were designed for use with each identical interrupter mechanism. The relevant design parameters chosen for each bent-beam actuator are shown in Table 4-2. Since the parameters were based on previously optimized bent-beam actuators, it is expected that the performance will be similar to what was shown in Table 4-1.

4.4.2 Force Measurement Technique

In addition, to designing a few stand-alone variations of the bent-beam electrothermal actuators for characterization testing, a few sets of actuators were designed with adjacent force measuring structures to determine the output force. The force

Table 4-2. Summary of the bent-beam actuator design parameters chosen for each of the interrupter mechanisms fabricated as part of this research effort.

Interrupter No.	Arm Length × No. of Arm Pairs	Actuator Thickness (μm)	Pre-Bend Angle (Degrees)	Arm Width (μm)	Tapered (Yes/No)
1	$400~\mu m \times 8~arm$	3.5	1.05	3.0	No
2	400 μm × 12 arm	3.5	1.05	3.0	No
3	400 μm × 8 arm	3.5	1.05	3.0	Yes

measuring structures are essentially simple cantilever beams that are positioned perpendicular to the direction of the actuator's motion [13]. Figure 4-15 shows an illustration of this arrangement. By definition, a cantilever beam is rigidly fixed at one end and free to move at the other end when a load is applied somewhere along its length. For simplicity, the applied load was designed to be located at the end of the cantilever beam. To accomplish this, one end of the actuator's coupling beam was extended so that it could be placed adjacent to the beam's tip. This arrangement enabled the use of relatively simple formulas for an end-loaded cantilever beam. Figure 4-16 shows the specific cantilever beam arrangement used for this experiment.

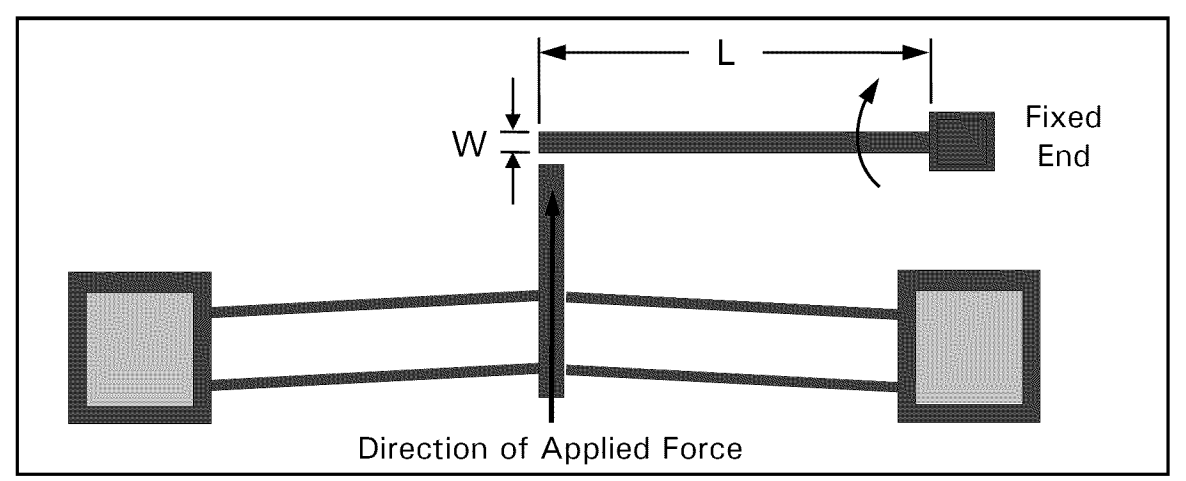


Figure 4-15. Illustration of actuator and cantilever beam arrangement for experimentally determining applied force. The length of the beam, L, and the width of the beam, w, are also shown.

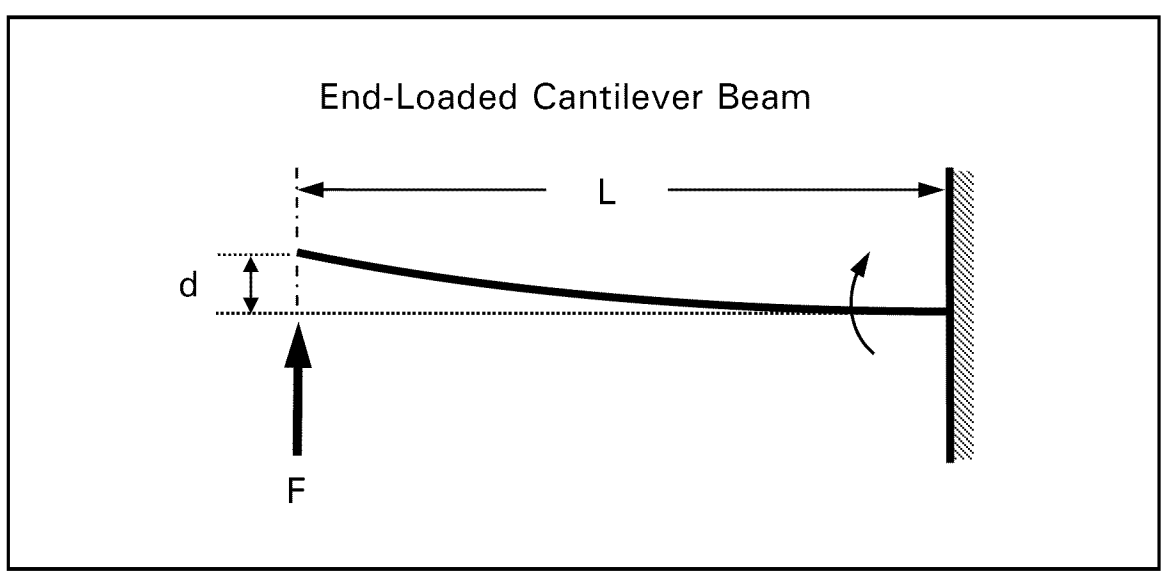


Figure 4-16. Schematic of an end-loaded cantilever beam arrangement used to determine the applied force from the bent-beam actuators [21]. The length of the beam, L, the applied force, F, and the deflected distance, d, are shown.

The equation that describes the maximum deflection of the cantilever beam, d_{max} , due to an applied force, F, at the tip of the beam is [21]:

$$d_{\text{max}} = \frac{F \cdot L^3}{3 \cdot E \cdot I} \quad (\mu \text{m}) \tag{4.5}$$

where

 $L = length \ of \ the \ beam \ (\mu m)$

E = Young's modulus (GPa)

 $I = moment \ of \ inertia \ (\mu m^4)$

The polysilicon deposited by the PolyMUMPs process has a Young's modulus of 158 ± 7.9 GPa, as reported by Sharpe et al. This value varies widely throughout the literature; however, the extensive mechanical testing performed to obtain the above value provides the largest level of confidence available, other than directly measuring it for each fabrication run. In addition, Sharpe et al. showed that there was very little variance in Young's modulus for polysilicon samples provided by three separate fabrication processes [22].

Considering that the cantilever beam has a rectangular cross-sectional area, the moment of inertia is given by [21]:

$$I = \frac{t \cdot w^3}{12} \quad (\mu \text{m}^4) \tag{4.6}$$

where

$$t = thickness of the beam$$
 (µm)
 $w = width of the beam$ (µm)

Thus, by combining Equation (4.5) and Equation (4.6), the following relationship for the applied force, F, on the cantilever beam, when maximum deflection has occurred, is:

$$F = \frac{E \cdot t \cdot w^3 \cdot d_{\text{max}}}{4 \cdot I^3} \quad (\mu \text{N})$$
 (4.7)

Therefore, to experimentally determine the applied force, the actuator is powered thereby causing the coupling beam tip to move toward the free end of the cantilever beam. After contact is made, the load applied to the beam forces it to bend about its fixed end. When the beam has reached its maximum deflection, the deflection distance, d_{max} , is recorded and used in Equation (4.7) to determine the force applied by the actuator. Note that this force value does not represent the total force capacity of the actuator, but rather the force applied to the beam at the instance maximum *beam* deflection has occurred [8]. Moreover, using this method assumes that any effects due to friction are negligible [11].

The cantilever beams used for this experiment were fabricated in the same materials (Poly1 + Poly2) as the bent-beam actuators. Hence, both the actuators and the beams are designed to have a thickness of 3.5 µm. This theoretically implies that, upon release, both structures will likely be lined up at the same physical height, thus reducing any negative effects that might arise due to out-of-plane bending (e.g., the actuator

"jumping" over the cantilever beam as resistance is encountered). Furthermore, the initial separation between the actuator and the cantilever beam is designed to be approximately 2 μ m, which is close enough to enable solid contact, but far enough away to ensure the two structures are indeed separated during fabrication. For example, if any mask misalignments occur, a spacing of less than 2 μ m could cause the two structures to be fabricated as one structure, thus prohibiting performance of the force measuring experiment.

Additionally, the width of the cantilever beam had to be considered. It was reported in Sinclair that if the force measuring beams are not stiff enough to sufficiently resist the load applied by the actuator, maximum deflection will never occur and a valid force measurement value cannot be obtained [8]. Consequently, the widths of the cantilever beams were chosen to be 8 µm. Lastly, three different beam lengths (100 µm, 200 μm, and 300 μm) were designed for each variation of the bent-beam actuators. This was done to ensure maximum deflection data could be accurately obtained. For instance, as alluded above, the beam stiffness needs to be within a certain range to ensure that maximum deflection of the beam occurs before the actuator's deflection limit is reached. This limit is typically around 15 µm for the majority of u-shaped and bent-beam electrothermal actuators. If the beams are excessively short, they could be too stiff and the actuators may be unable to produce any measurable beam deflection. Alternatively, if the beams are excessively long, maximum deflection of the beam may never occur within the actuator's deflection range. Figure 4-17 shows a graphical representation of Equation (4.5), depicting the actuator force required to produce maximum deflection for a cantilever beam with three different lengths and the following parameters in common:

E=158 GPa, t=3.2 µm, and w=8 µm. Notice that for the beam length of 100 µm, a force of 200 µN is required to produce a maximum deflection of about 3 µm. In addition, recognize that for a specific force output (dependent on the design parameters of a given actuator), the optimal cantilever beam length should result in a maximum deflection of less than 15 µm, which is the approximate limit of the bent-beam actuators. If the beam is designed such that maximum deflection occurs above this limit, it will not be observed, and the output force will be unmeasurable. However, the output force is usually not known prior to testing, so the best approach is to design cantilever beams with multiple lengths, such that the predicted maximum deflection falls within a reasonable and measurable range.

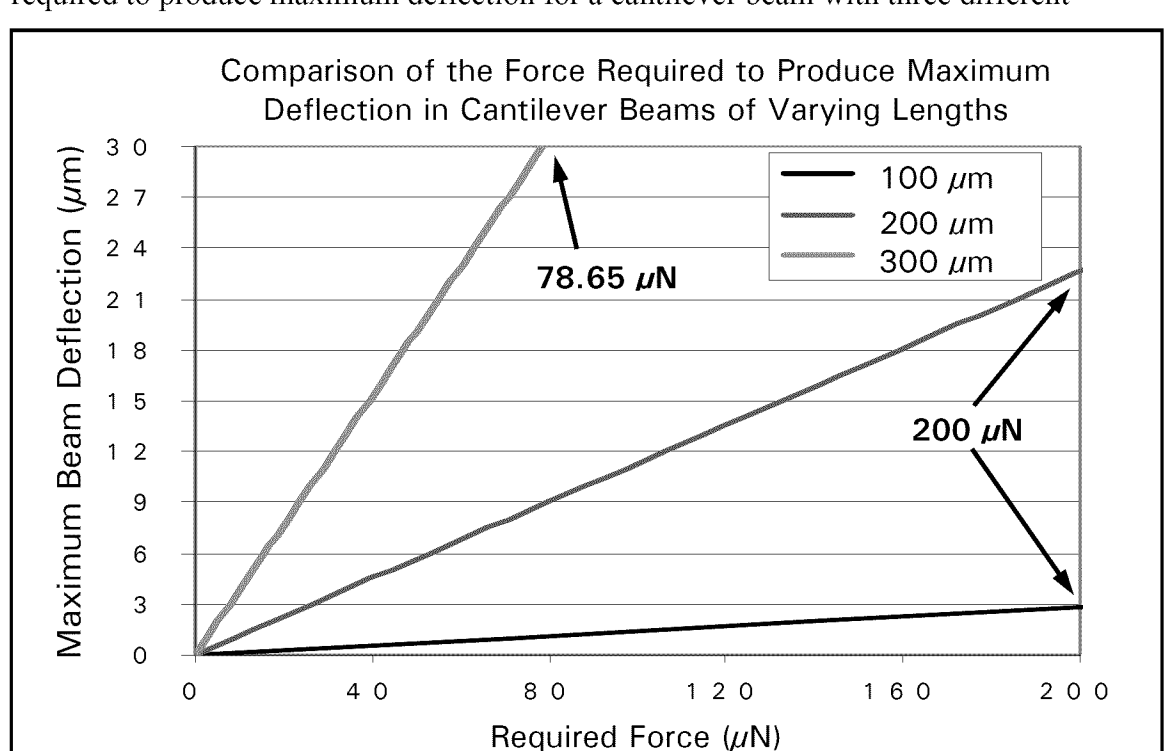


Figure 4-17. Graphical representation of Equation (4.5), depicting the actuator force required to produce maximum deflection for a cantilever beam with three different

lengths and the following common parameters: E = 158 GPa, t = 3.2 µm, and w = 8 µm.

4.5 Interrupter Design Theory

The theoretical design of the interrupter mechanism presented in this thesis focuses on the means to interrupt the flyer, of a solid-state slapper detonator, so that it is prevented from initiating a HE pellet in the explosive train. Alternatively, it is just as important to allow the flyer to pass through the interrupter mechanism when a valid launch condition is present. The approach taken to perform the interrupting function was to arrange four moveable plates in an overlapping pattern in an effort to provide additional interruption strength than could otherwise be provide by only two plates. Figure 4-18 shows the arrangement of the four separate interrupter plates. Both Poly1 (bottom) and Poly2 (top) were used to create the overlapping pattern.

Additionally, each of the four interrupter plates is physically joined to its own bent-beam electrothermal actuator by a linkage beam that directly translates the actuator's motion to the plate. The operation of the bent-beam electrothermal actuators is described in section 4.4. The arrangement between the actuator and its interrupter plate is such that when the actuator moves linearly outward, the small initial aperture created between the four interrupter plates expands, providing an opening that the flyer material can pass through on its path to the HE pellet.

Finally, a latching structure was designed to provide a method for locking the opened aperture. The latches function by the mating of two initially separated components. The first component is the triangular-tipped extension protruding from the deflection end of the actuator's coupling beam, and the second component is a fixed structure with two flexible locking beams that extends towards the first component. Upon activation of the actuator, the triangular-tipped extension of the actuator moves

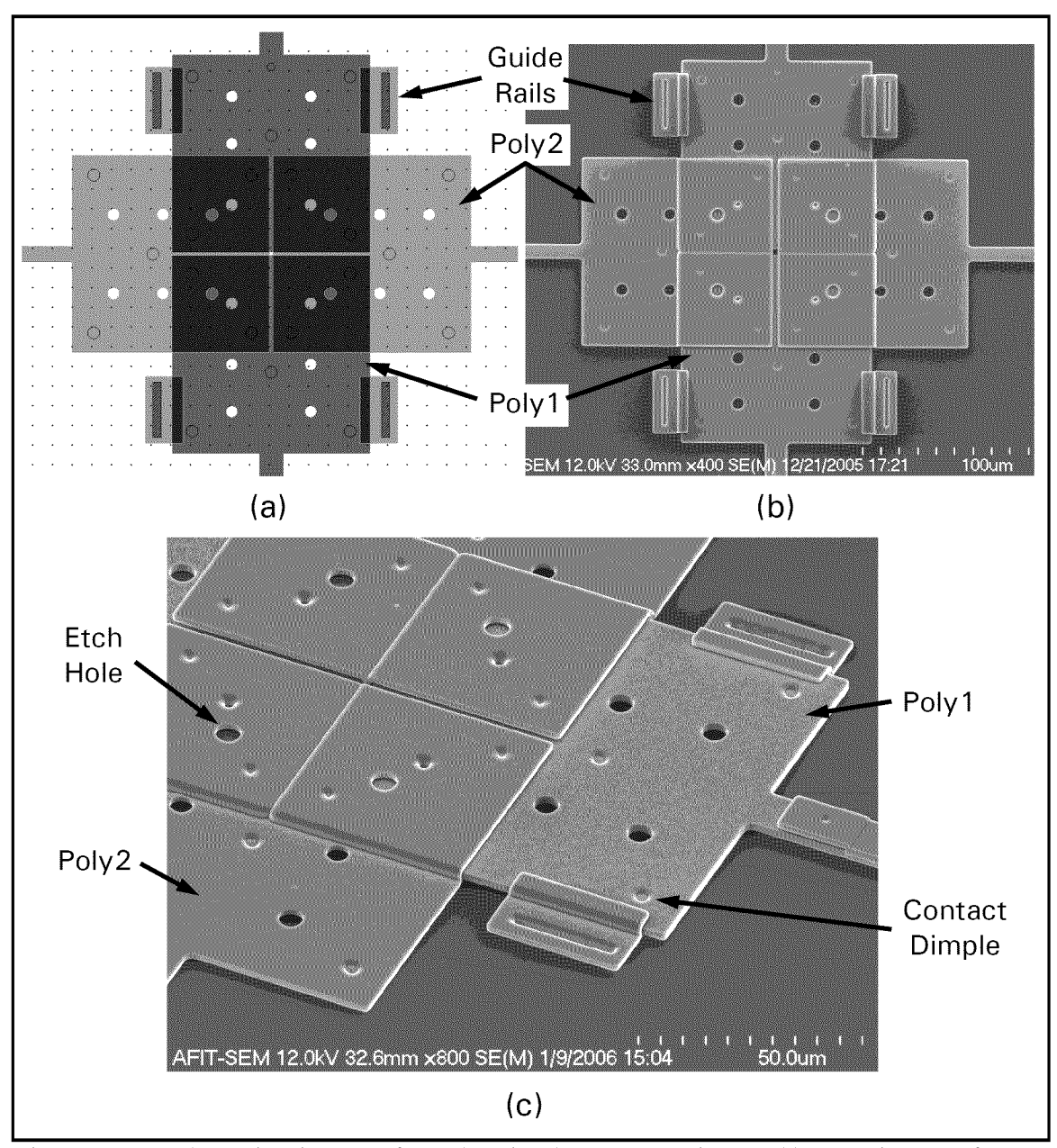


Figure 4-18. (a) Design layout of overlapping interrupter plates. (b) SEM image of fabricated overlapping interrupter plates. (c) SEM image of overlapping interrupter plates showing conformal topology.

toward the fixed component. When the two components come in contact with each other, the flexible beams will move perpendicular to the motion of the actuator (due to the applied force) and mating occurs when the triangular tip completely passes the tip of the flexible beam. Figure 4-19 shows two SEM images of the fabricated latching structure.

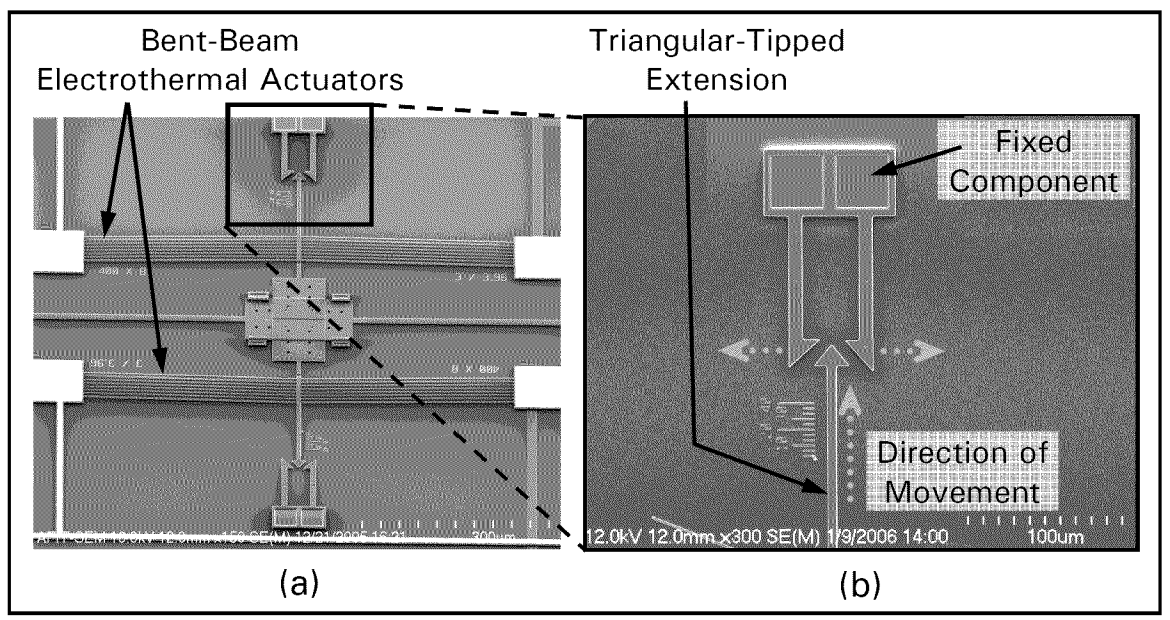


Figure 4-19. SEM images showing (a) the connections between the latching mechanism and the actuator, and (b) the two components which make up the latching mechanism.

It is important to note that using this latching method requires that the desired latching distance be pre-determined, since the distance between the two locking components is fixed after fabrication.

4.5.1 Analysis of Interrupter Aperture

The interrupter aperture is produced by the overlapping arrangement of the four fabricated square plates. Initially, the plates are designed to be in a closed, or safe, position in order to prevent the flyer material from initiating the HE pellet. However, because of the spacing constraints discussed in section 4.1.2, the two Poly1 plates and the two Poly2 plates are designed to have an initial separation of 2 μ m. This prevents the possibility of having the two plates (Poly1-to-Poly1 and Poly2-to-Poly2) fused together due to any mask misalignments that could occur in the PolyMUMPs process. Consequently, in the initial "closed" position, there is a small 4 μ m² opened area as shown in Figure 4-20.

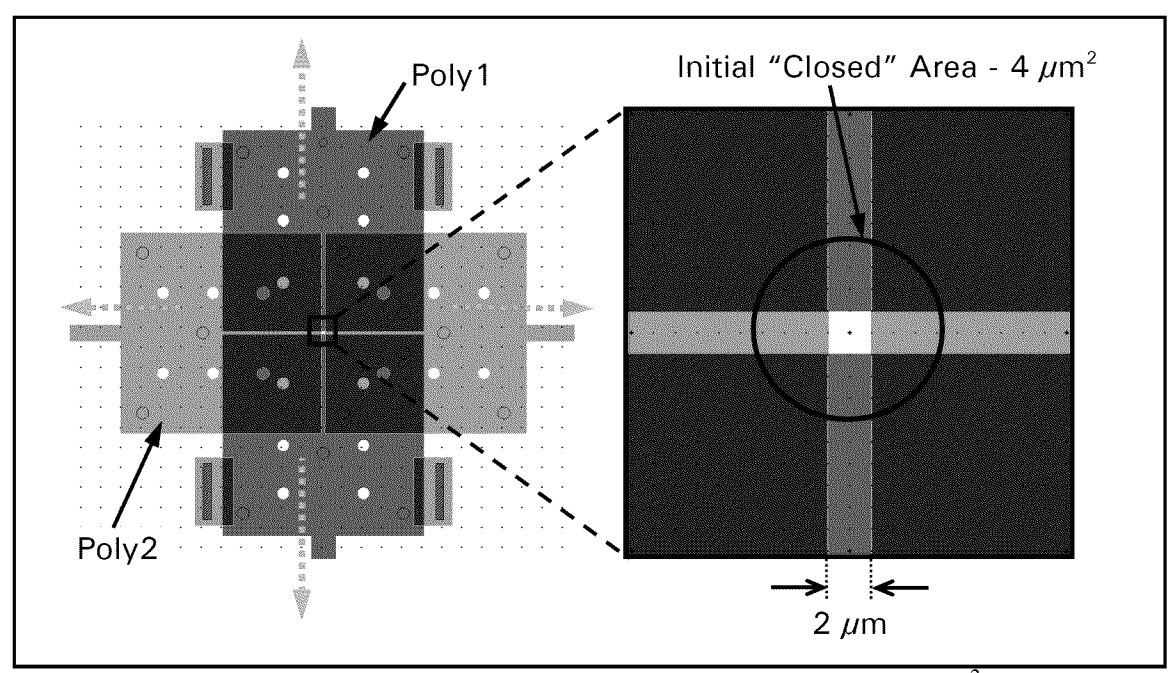


Figure 4-20. Design layout of the "closed" interrupter, depicting the $4-\mu m^2$ area where no coverage exists.

When the actuators are powered, the interrupter plates will move outward, as shown by the green arrows in Figure 4-20. This causes the area of the aperture to rapidly expand, up to a limit resulting from the maximum deflection of the bent-beam actuators. Since each actuator is designed to the same exact design parameters (see Table 4-2), it is reasonable to assume they will all deflect exactly the same distance for a given applied power (i.e., when one actuator deflects 1 μ m, all the other actuators also deflect 1 μ m). This trend should continue until maximum deflection is reached, resulting in the aperture area being maximized. Consequently, the following relationship is used to describe the entire area of the aperture, A_a , as a function of a single actuator's deflection distance, d:

$$A_a = (2 \cdot d + 2)^2 \quad (\mu \text{m}^2) \tag{4.8}$$

Figure 4-21 shows an illustration of this change in aperture area as a result of actuator deflection. Notice that a small actuator deflection has a rather large affect on the aperture area in accordance with Equation (4.8). In addition, Figure 4-22 shows the graphical representation of Equation (4.8), which shows the quadratic increase in the aperture area as a function of actuator's deflection. From this graph, an aperture area of $1444 \ \mu m^2$ is expected for the interrupter mechanism designed for this thesis, based on the anticipation of obtaining a reasonable actuator deflection of 18 μm . Accordingly, if this conceptual interrupter mechanism is integrated with a solid-state slapper detonator, the ejected flyer material must have a cross-sectional area of less than $1444 \ \mu m^2$, so that it can pass through the aperture and initiate the HE pellet.

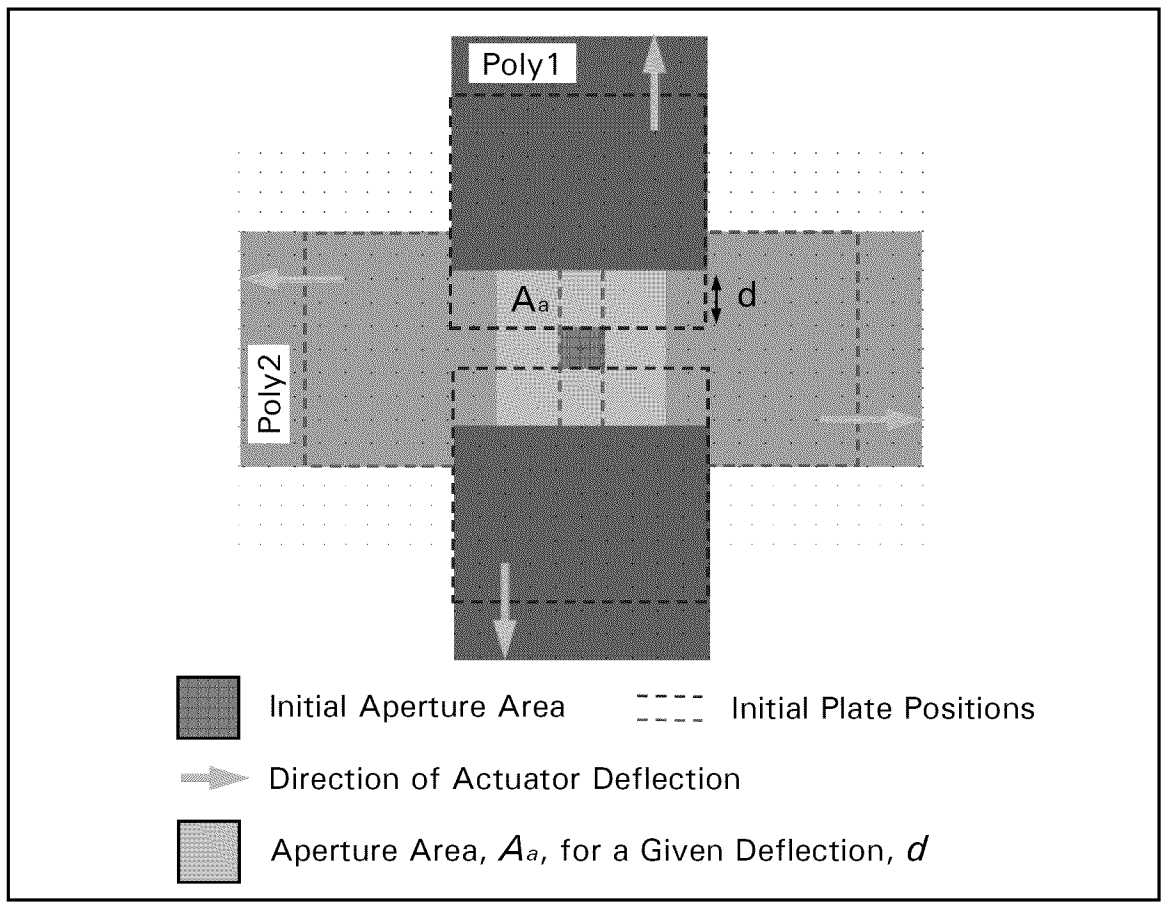


Figure 4-21. Illustration of the change in aperture area as a result of actuator deflection. Notice the difference between the initial aperture area and the resulting aperture area.

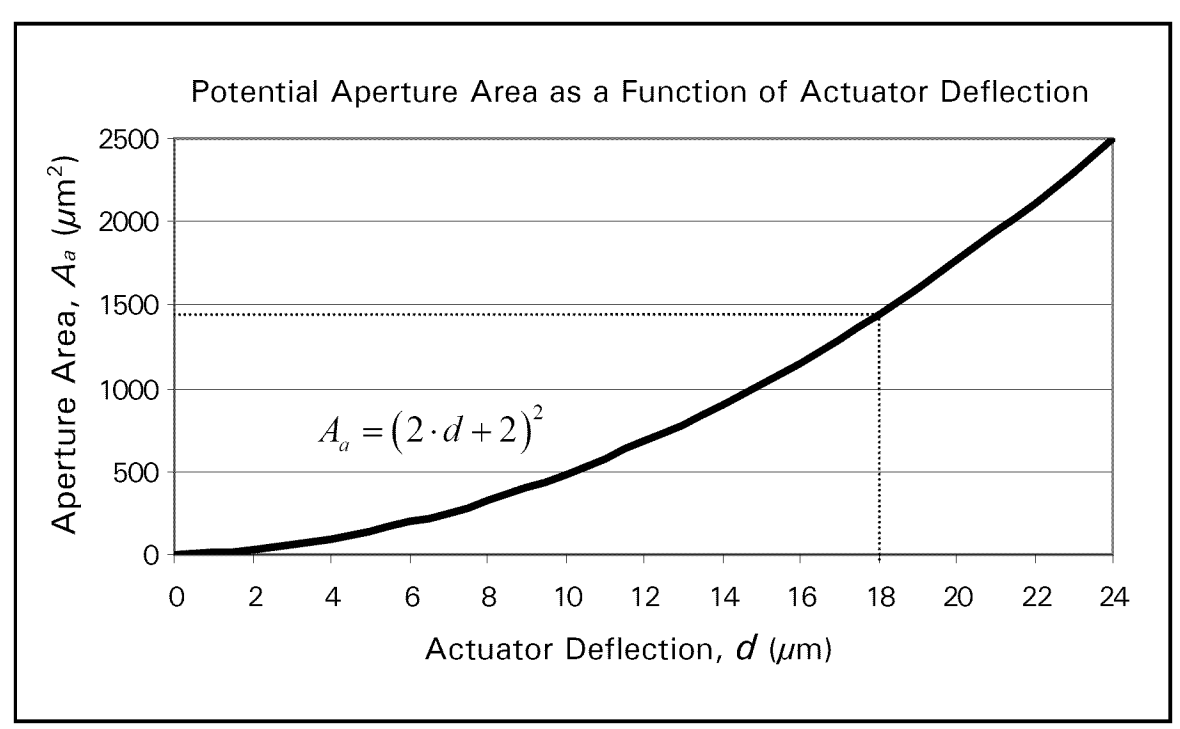


Figure 4-22. Graphical representation of the quadratic dependence of the actuator deflection on the aperture area in accordance with Equation (4.8). The red line indicates a realistic expectation for the aperture area based on the anticipated performance of the bent-beam actuators designed for the interrupter mechanism in this thesis.

4.5.2 Required Actuator Force Calculations

To determine the force required to move all the elements attached to the bent-beam actuators, a simple free-body diagram was constructed. Figure 4-23(a) shows one of the actuator elements that make up the complete interrupter mechanism. The element shown consists of a Poly2 interrupter plate, the Poly2 linkage, and the Poly1 + Poly2 latching beam component attached to the actuator. Even though this figure only shows one actuator element, this analysis can be easily repeated for the Poly1 interrupter plate, with slight modifications.

Figure 4-23(b) shows the free-body diagram corresponding to the element in Figure 4-23(a). The normal force, N, can be determined by:

$$N = m_T \cdot g = V_T \cdot \rho \cdot g \quad (N) \tag{4.9}$$

where

$$m_T$$
 = total mass of all components (kg)
 g = acceleration due to gravity (m/s²)
 V_T = total volume of all components (m³)
 ρ = density of polysilicon (kg/m³)

Once the normal force is known, the actuator force, F, can be calculated by referring to the free-body diagram and observing the relationship of:

$$F = f_s = \mu_s N \quad (N) \tag{4.10}$$

where

$$f_s$$
 = static friction force (N)
 μ_s = coefficient of static friction (dimensionless)

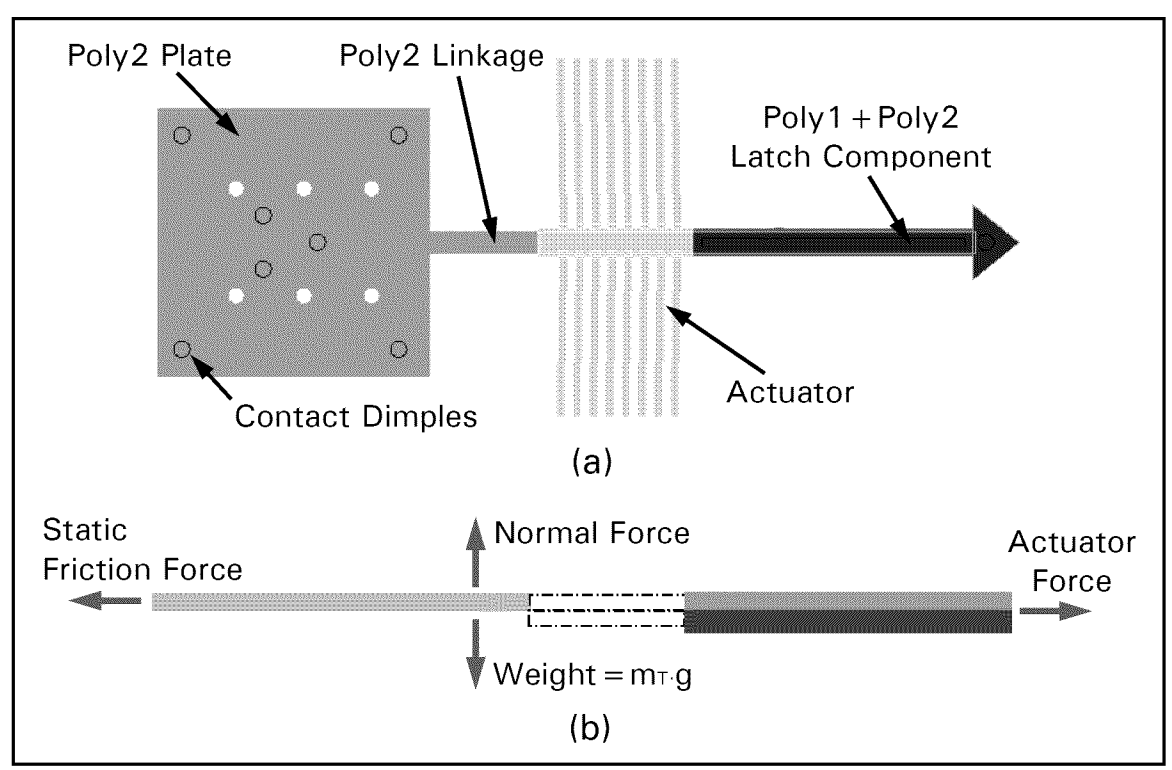


Figure 4-23. (a) One of the four actuator elements that make up the interrupter mechanism. The actuator is dimmed since it is not included in the free-body diagram. (b) Free-body diagram of the interrupter mechanism shown in (a). Only the (Poly1) plate, the linkage, and the latch component are considered in determining the required actuator force.